# Tracking Inhibitory Alterations during Interstrain *Clostridium difficile* Interactions by Monitoring Cell Envelope Capacitance

Yi-Hsuan Su,[†] Ali Rohani,[†] Cirle A. Warren,[‡] and Nathan S. Swami*,[†]

[†]Department of Electrical & Computer Engineering and [‡]Infectious Diseases, School of Medicine, University of Virginia, Charlottesville, Virginia 22904, United States

Ⓢ *Supporting Information*
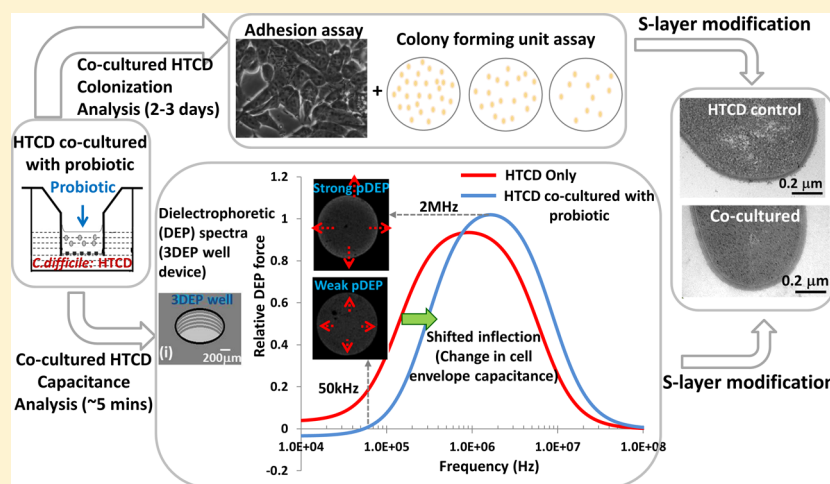
ABSTRACT: Global threats arising from the increasing use of antibiotics coupled with the high recurrence rates of *Clostridium difficile* (*C. difficile*) infections (CDI) after standard antibiotic treatments highlight the role of commensal probiotic microorganisms, including nontoxigenic *C. difficile* (NTCD) strains in preventing CDI due to highly toxigenic *C. difficile* (HTCD) strains. However, optimization of the inhibitory permutations due to commensal interactions in the microbiota requires probes capable of monitoring phenotypic alterations to *C. difficile* cells. Herein, by monitoring the field screening behavior of the *C. difficile* cell envelope with respect to cytoplasmic polarization, we demonstrate that inhibition of the host-cell colonization ability of HTCD due to the S-layer alterations occurring after its co-culture with NTCD can be quantitatively tracked on the basis of the capacitance of the cell envelope of co-cultured HTCD. Furthermore, it is shown that effective inhibition requires the dynamic contact of HTCD cells with freshly secreted extracellular factors from NTCD because contact with the cell-free supernatant causes only mild inhibition. We envision a rapid method for screening the inhibitory permutations to arrest *C. difficile* colonization by routinely probing alterations in the HTCD dielectrophoretic frequency response due to variations in the capacitance of its cell envelope.

KEYWORDS: *bacteria, Clostridium difficile, capacitance, dielectrophoresis, diagnostics, microfluidics*

The role of human microbiota in health and disease is becoming increasingly apparent, but optimizing microbial interactions to reduce infections is challenging. *Clostridium difficile* (*C. difficile*) infection (CDI), a toxin-mediated intestinal disease that is the single most common cause of antibiotic-induced in-hospital enteric infection, is a perfect example. It is caused by *C. difficile*, a Gram-positive, spore-forming anaerobic bacteria, upon the elimination of healthy microflora in the gut under the administration of broad-spectrum antibiotics.[1] Metronidazole and vancomycin are the most commonly used antibiotics for CDI treatments. However, CDI rates continue to see steady rises worldwide,[2] with increasing incidences of treatment failure due to disease recurrence with the same strain after standard antibiotic

treatments.[3] An alternate means to cause the inhibition of highly toxigenic *C. difficile* (HTCD) strains is through the application of probiotic microorganisms,[4] but the inhibitory permutations have not been optimized. For example, it has been shown that some lactic acid bacteria and yeast can significantly protect hamsters and mice from diarrhea and enterocolitis as well as lower tissue damage triggered by *C. difficile*.[5,6] Furthermore, *Bifidobacterium* and *Lactobacillus*, either in the form of supernatants or in co-culture, can inhibit *C. difficile* growth, cytotoxicity, and adhesion ability to human enterocyte cell lines.[7−10] Nontoxigenic *C. difficile* (NTCD)
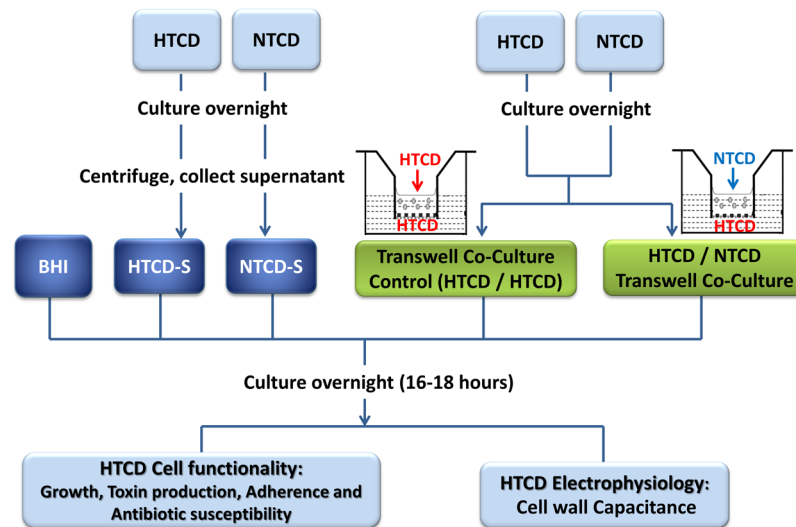
Figure 1. Experimental design for studying the inhibitory effects of nontoxigenic *C. difficile* (NTCD) on highly toxigenic *C. difficile* (HTCD).

strains, which do not produce toxin A or toxin B because of the absence of the pathogenicity locus (PaLoc), are typically not implicated in symptomatic CDI. Because NTCD strains are likely to compete with HTCD strains for similar colonization niches,[11−13] antagonistic interstrain interactions are envisioned. Prior studies have shown that gastrointestinal colonization of patients and hamsters by NTCD strains can reduce the incidence of CDI from HTCD strains.[13] Recent clinical trials have demonstrated the safety and efficacy of NTCD in healthy subjects and CDI patients.[11,12] The administration of NTCD strains as a probiotic to arrest primary and recurrent CDI is potentially preferable to current approaches based on fecal microbiota transplantation (FMT) that require time-consuming procedures for the preparation and maintenance of frozen capsulized FMT,[14] with poorly characterized microbial compositions that can have adverse effects.

Current methods to judge the inhibitory effect of probiotic microorganisms on *C. difficile* are based on animal model studies and in vitro adhesion assays with host cells. These are time-consuming and cumbersome and provide only indirect evidence of the inhibition, thereby limiting the inhibitory permutations that can be studied. S(Surface)-layer proteins, which form a part of the cell wall within both Gram-positive and Gram-negative bacteria, are integral in surface recognition, colonization, host−pathogen adhesion, and virulence.[15] A number of studies have shown that variations of the S-layer between *C. difficile* strains affect their colonization behavior.[16−18] In fact, because S-layer proteins from NTCD strains are known to effectively block the adherence of HTCD strains to host cells,[16] we use this inhibitory interaction to develop a probe for rapidly monitoring alterations in the HTCD cell envelope by tracking its capacitance. The high eccentricity ellipsoidal shape of *C. difficile* causes its strong polarization under electric fields, thereby making it a unique cell type for sensitive measurements of alterations in the capacitance of its cell envelope, based on the level of screening of cytoplasmic polarization. Specifically, we choose the HTCD strain, VPI10463, because it exhibits a significantly higher cell envelope capacitance than other common *C. difficile* strains with low or no toxigenicity (ATCC630 or VPI11186),[19] presumably because of its distinct S-layer composition that increases its cell wall roughness. The higher starting capacitance

level for this HTCD strain enables a significant dynamic range for its systematic reduction due to gradual alterations in its cell envelope during co-culture with the NTCD strain, VPI11186, which has a 3-fold-lower capacitance. In this manner, capacitance measurements on the HTCD cell envelope can be correlated to alterations in its functionality after co-culture, as validated by time-consuming adhesion assays and low-sensitivity toxin immunoassays, so that capacitance can serve as a rapid monitoring tool for optimizing the inhibitory interactions of various probiotics on this and other relevant HTCD strains.

In this study, rapid and contactless monitoring of the alterations in the cell envelope capacitance is accomplished by dielectrophoresis (DEP) and verified by electrorotation (ROT). DEP causes the frequency-selective translation of polarized bioparticles under a spatially nonuniform electric field, either toward (by positive DEP or pDEP) or away (by negative DEP or nDEP) from the high-field region, depending on the polarizability of the bioparticle versus that of the medium.[20,21] Hence, field screening caused by the cell envelope to its cytoplasmic polarization can be sensitively measured by DEP frequency spectra.[22,23] ROT is a complementary technique that measures the dipole relaxation behavior of cells under phase-shifted fields on the basis of their cofield and counter-field rotational frequency spectra.[24] Although DEP spectra directly reflect the relative differences in the degree of polarization between particles to enable their frequency-selective separation, ROT spectra reflect differences in dipole relaxation to better discern the frequency values at which the polarization dispersion shows significant inflections because these show up as maximum or minimum rotational values.[25] In prior work,[19] we demonstrated that the systematic differences in cell wall morphology between particular *C. difficile* strains can significantly shift their DEP crossover to enable their frequency-selective DEP separation. Herein, we focus on probing interactions between particular *C. difficile* strains within various types of co-cultures by discerning the DEP spectral shifts and fitting the spectra to an ellipsoidal two-shell model (with the cell wall and membrane as shells) to quantify alterations in the capacitance of the HTCD cell envelope. These alterations in cell envelope capacitance are found to be strongly correlated to morphological differences in the cell

envelope as observed by electron microscopy and to the HTCD colonization ability as judged by its adherence to host cells. We envision that cell envelope capacitance measurements on HTCD can serve to rapidly screen for the particular probiotic combinations that arrest the colonization ability of co-cultured HTCD versus current methods based on cumbersome adhesion assays.

■ MATERIALS AND METHODS

The approach to examining alterations in the functionality and electrophysiology of HTCD either cultured within a cell-free NTCD supernatant (henceforth NTCD-S) or co-cultured with NTCD in a transwell with a 0.4 μm pore size membrane to separate the cultures (henceforth transwell co-culture) is shown in Figure 1.

Preparation of Bacterial Co-Cultures. High toxigenic (VPI10463, HTCD) and nontoxigenic (VPI11186) *C. difficile* strains (purchased from ATCC) were cultured in brain heart infusion (BHI) broth (BD, BBL BHI) at 37 °C overnight in an anaerobic chamber. For supernatant culture, the overnight cultured cells (O.D. 600 = 0.89 ± 1%) were centrifuged at 3000 g for 5 min. The residual cells in the supernatants were removed by a 0.2 μm pore size filter (Millipore). The supernatants were freshly prepared before each experiment. Pelleted HTCD or NTCD cells were resuspended in fresh BHI. The HTCD suspension (200 μL) was inoculated in 800 μL of the respective supernatants (BHI, HTCD supernatant or NTCD supernatant, O.D. 600 = 0.331 ± 1%). For transwell co-culture, 200 μL of the HTCD suspension and 1.2 mL of BHI were inoculated in the wells within a 12-well plate for co-culture with 200 μL of NTCD or HTCD suspensions (co-culture control) and 600 μL of BHI inoculated in the transwell insert. The cells inoculated in supernatants or in the transwell co-culture setup were incubated at 37 °C overnight (16−18 h) in an anaerobic chamber. Prior to the DEP or ROT, the medium was replaced with 8.8% sucrose water, with medium conductivity (Mettler Toledo FE20) of 5 ± 5% mS/m as adjusted by the BHI medium. Using the colony-forming unit (CFU) assay, we confirmed (Supporting Information Table S1) that *C. difficile* can survive for up to 3 h under the aerobic conditions within this altered medium (typical time frame for DEP and ROT analysis is <5 min).

Host-Based Adherence Assay. As per standard protocol,[19] the human colon epithelial cell line, HCT-8 (ATCC), was used as the host cell in this assay. HCT-8 cells were grown as a confluent monolayer in 6-well plates prior to the assay. Overnight *C. difficile* cultures were pelleted and resuspended in fresh BHI medium and were adjusted to equal concentration levels by optical density measurement (Eppendorf biophotometer). An equal concentration of each culture condition was added to each well, and the plates were incubated in the anaerobic chamber at 37 °C for 3 h. After 3 h, nonadhered *C. difficile* cells were eliminated by three washing steps with PBS. Finally, adhered *C. difficile* cells were harvested and were enumerated by CFU assay. Each experiment was performed in triplicate and repeated with three different HCT-8 cell passages.

Growth Measurement. The optical density (O.D.) at 600 nm wavelength for cells inoculated in supernatants or within the transwell co-culture was measured by spectrophotometry (Eppendorf biophotometer). After overnight culture (16−18 h) under each condition, aliquots of 50 μL were used for growth measurement in a disposable cuvette. The O.D. of each supernatant was compared to the BHI control (normalized at 100%), and the O.D.s of HTCD co-cultures were compared to the co-culture control (HTCD on either side of a transwell plate), which was normalized to 100%.

Enzyme-Linked Immunosorbent Assay for Toxin Levels. Total toxin (A/B) production was measured using the *C. difficile* TOX A/B II kit (TechLab). Culture supernatants were collected by centrifugation at 3500 rcf for 5 min and stored at −20 °C. The A450 values of supernatants were compared to the BHI control as 100%, or the A450 values of NTCD and the HTCD transwell co-culture were compared to the co-culture HTCD-only control as 100%.

Dielectrophoretic Characterization of *C. difficile*. DEP measurements were conducted on a 3DEP dielectrophoretic analyzer (DEPtech, Uckfield, U.K.) with a recording interval set to 30 s at 10 V_{pp}, with data collected over 20 points between 50 kHz and 45 MHz. The average relative DEP force at each frequency was obtained by analyzing at least five different measurements, and results were repeated three times with each new batch of cells.

Image Analysis on DepTech's 3DEP Reader. In the DepTech 3DEP reader, an electric field is applied using gold-plated conducting electrode stripes inside the wall of each well (Figure 4a(i)), and the DEP response is measured at 20 different frequencies applied to the individual wells. The level of DEP at each frequency is obtained by analyzing spatiotemporal variations in light intensity from particle scattering using particular bands in each of the 20 wells, after normalization to the background at zero field (time = 0), by accounting for the electric field distribution in the wells.[26] These normalized weighted changes in light intensity are used to measure the relative DEP force at each frequency[27,28] (details in S3 SI). For ellipsoidal particles of high eccentricity (large major/minor axis ratio) such as *C. difficile*, the particle undergoes electro-orientation as soon as the electric field is applied. Upon field application in the wells, the particles orient along the field lines, causing the major axis of the cell to be oriented to the field. This causes a dramatic and rapid accumulation of the light intensity in the well (Figure 4a(ii),b), thereby obscuring light intensity alterations due to DEP behavior because the subsequent light intensity is usually normalized to the intensity at zero time. Hence, this problem was addressed by identifying the particular time frame following the electro-orientation of cells and using this as the baseline for normalizing the light intensities from later frames (Figure 4a(ii),b). After 30 s of field, positive DEP was clearly apparent (Figure 4a(iii),c). The light intensity in Figure 4c was normalized to that in Figure 4b. The DEP spectra were obtained by analyzing the alteration of light intensity, only in the regions closer to the edges (from bands 6−9) to avoid interferences from the electro-orientation of cells in the central region (from bands 1−5), which has a lower electric field intensity than the edge region.

Computing Dielectric Properties from DEP Spectra. The DEP spectra of *C. difficile* after various co-cultures were correlated to dielectric parameters (permittivity or ε and conductivity or σ) to compute alterations in the electro-physiology of particular intracellular regions (outer insulating envelope denoting the cell wall and membrane versus the inner conducting cytoplasm).[25] For this purpose, an ellipsoidal two-shell dielectric model,[29,29,30] denoting the shells formed by the cell wall and membrane to the cytoplasmic core of *C. difficile*, was used to compute ε_{wall}, σ_{wall}, $\varepsilon_{membrane}$, $\sigma_{membrane}$, ε_{cyto} and σ_{cyto}, as described within Supporting Information S5. The diluted BHI medium was assigned $\varepsilon_{medium} = 80$,[20] and σ_{medium} was

measured to be 5 mS/m. Geometrical information about the cell axis and cell wall thickness was obtained from TEM images. The membrane thickness, which is not resolved from the images, was computed from the literature[31,32] (Table S2 in Supporting Information). Using the fitted dielectric values and thickness (t) of the cell wall and membrane, the cell envelope capacitance was computed as[33]

$$C_{\text{envelope}} = \frac{\varepsilon_{\text{wall}}\varepsilon_{\text{membrane}}}{\varepsilon_{\text{wall}}t_{\text{membrane}} + \varepsilon_{\text{membrane}}t_{\text{wall}}} \tag{1}$$

Electrorotation of *C. difficile*. Electrorotation was measured on a chip with planar hyperbolic-shaped gold electrodes arranged within a quadrapole pattern on coverslip glass with a fluidic cell, as per our prior work[25] (details in S4 of Supporting Information). Individually soldered electrical connections allowed for the independent energization of electrodes. A four-channel arbitrary waveform generator (TGA12104−Thurlby Thandar Instruments) was programmed to apply 90° phase-shifted signals to adjacent electrodes. Electrorotation of the *C. difficile* cells was observed under a Zeiss Z1 microscope and recorded with a Hamamatsu CMOS camera at 100 fps (frames per second). The average rotation rate at each frequency was obtained by analyzing at least 15 cells, with results repeated at least 3 times with different batches of cells. Because multishell model fits to the imaginary portions of polarizability are not readily available for ellipsoidal particles, we focus on utilizing the counter-field ROT spectra to delineate the frequency of inflection to pDEP.

Transmission Electron Microscope Imaging. *C. difficile* samples cultured overnight (1 mL: O.D. 600 = 0.89 ± 1%) were pelleted and washed in PBS and fixed in 2% glutaraldehyde and 2% paraformaldehyde in PBS for 4 h at room temperature. The samples were pelleted and washed in DI water before resuspension in 2% osmium tetroxide for 30 min at room temperature and rewashed in DI water. The samples were dehydrated through a serial gradient ethanol solution (50, 70, 95, and 100%) for 10 min at each level. The samples were then resuspended in 1:1 EtOH/EPON (epoxy resin) overnight, followed by 1:2 EtOH/EPON for 2 h, 1:4 EtOH/EPON for 4 h, and 100% EPON overnight. After embedding the samples in fresh 100% EPON, the samples were baked in a 65 °C oven. The EPON-hardened samples were sectioned to 75 nm, mounted onto 200 mesh copper grids, and contrast stained with 0.25% lead citrate and 2% uranyl acetate for TEM imaging (JEOL 1230) at 80 kV (SIA digital camera).

RESULTS AND DISCUSSION

Inhibition of HTCD after Co-Culture with NTCD. The alterations in functionality of HTCD cultured within either a cell-free NTCD supernatant (henceforth called NTCD-S) or co-cultured with NTCD in a transwell plate, wherein the cultures are separated by a 0.4 μm pore size membrane (henceforth called transwell co-culture), are examined using standard microbiological analysis. The measured growth rates after the overnight culture of HTCD in various supernatants, including fresh BHI broth (positive control), cell-free HTCD supernatant (HTCD-S), and cell-free NTCD supernatant are normalized to the growth rate of the cells cultured in BHI broth (Figure 2a). For the analogous HTCD transwell co-culture with NTCD, a co-culture system with the HTCD inoculates on either side of the membrane serves as the so-called co-culture control. For HTCD cultured in HTCD-S and in NTCD-S, the
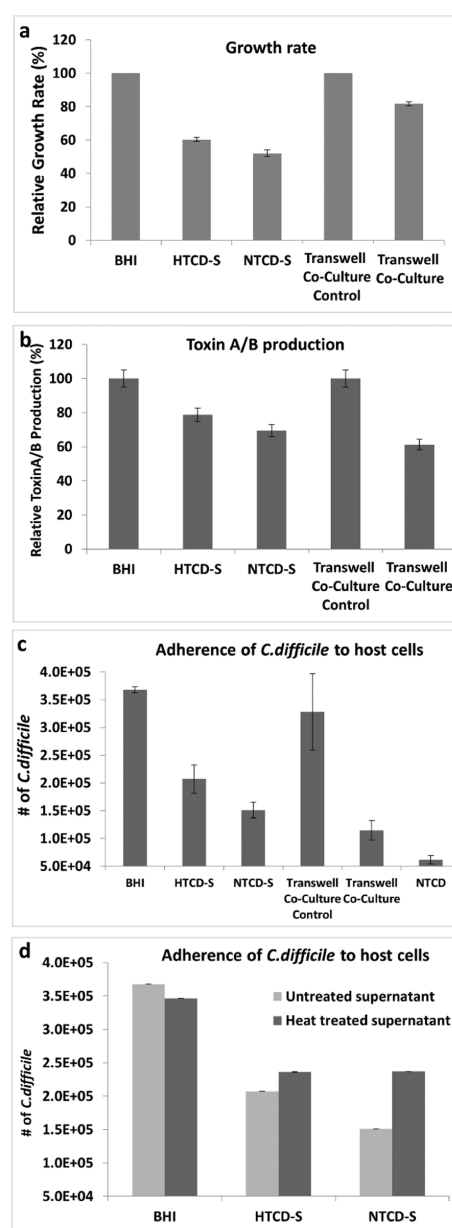
Figure 2. (a) Relative growth rate and (b) relative toxin production for HTCD after various culture conditions, with values for HTCD-S and NTCD-S normalized to those of the BHI control and the values for transwell co-cultured HTCD normalized to the transwell co-culture control. Variations in HTCD adherence to human colon epithelial cells, as enumerated by colony-forming units (CFU): (c) after each culture condition and (d) for HTCD cultured in heat-treated versus untreated NTCD supernatant.

growth rates are reduced to ∼60% of that obtained within BHI broth, which we attribute to the lack of sufficient nutrients for cell growth. The absence of significant differences in the growth rate between HTCD cultured in HTCD-S versus in NTCD-S suggests that the leftover nutrient levels in the HTCD-S and NTCD-S are quite similar. Although the NTCD-S does not significantly inhibit the growth of the HTCD, the growth rate after transwell co-culture of HTCD with NTCD is reduced to ∼80% of that of the co-culture control (Figure 2a). Toxin production levels show similar trends, with modest drops from the 100% level for the HTCD control (cultured in BHI) to almost equivalent levels of 80 and 70% for HTCD cultured in

HTCD-S and NTCD-S, respectively, whereas the toxin production for HTCD after transwell co-culture with NTCD drops to 60% of its value versus the co-culture control. For the transwell co-culture system, it is noteworthy that although the cell numbers are reduced by only 20% versus the control (Figure 2a), the toxin production level is reduced by 40% (Figure 2b), indicating that the inhibitory effect of HTCD after co-culture with NTCD extends well beyond their lower cell numbers versus the control, likely because of secreted extracellular factors during the co-culture. The role of this inhibitory effect on the colonization ability of HTCD is assessed by the standard adhesion assay. HTCD cells cultured in BHI show the highest adherence numbers, followed by HTCD cultured in HTCD-S, HTCD cultured in NTCD-S, and finally HTCD co-cultured with NTCD, which shows an adhesion level just slightly higher than that of a pure NTCD culture (Figure 2c).

These sharp differences in the degree of adherence to host cells versus those of the control confirm the inhibitory role of HTCD co-cultured with NTCD with respect to its colonization ability. Although lower host cell adherence for HTCD in HTCD-S versus the control (HTCD in BHI) may be attributed to the lack of nutrients (as apparent from the growth rates in Figure 2a), the HTCD cultured in NTCD-S, which has a level of nutrients similar to that of the respective culture in HTCD-S (as apparent from their similar growth rate in Figure 2a), shows much lower numbers of adherent bacteria, indicating the role of extracellular factors in the NTCD-S in inhibiting the adherence of HTCD to the host cells. To further examine the inhibition mechanism, the supernatants were heat-treated to denature any heat-sensitive factors. As per Figure 2d, there is a significant increase in host cell adherence for HTCD cultured within this heat-treated NTCD-S versus the respective culture in untreated NTCD-S. In fact, HTCD cultured within heat-treated NTCD-S shows equivalent adherence numbers to HTCD cultured in untreated HTCD-S, indicating the loss of inhibition ability of NTCD-S after heat treatment. Hence, the colonization inhibition of HTCD cultured in untreated NTCD-S is attributed to thermolabile extracellular factors present in the NTCD-S. Additionally, we infer that transwell co-culture with NTCD has a greater inhibitory influence on HTCD versus culture in NTCD-S because in the former the growth rate is mildly reduced, the toxin levels are more sharply reduced, and the colonization ability is drastically decreased. In the latter case, the inhibitory effect extends only to a reduction in the colonization ability of the HTCD strain. Although HTCD cells in the co-culture system with NTCD are in dynamic contact with freshly secreted extracellular factors, this is not so for the HTCD culture in cell-free NTCD supernatant, where the contact is with isolated extracellular factors from one particular time point, thereby explaining the greater inhibition within the former system.

Monitoring the Cell Envelope Capacitance by Dielectrophoresis. In previous work, we correlated differences in the cell wall roughness of particular *C. difficile* strains to systematic variations in their crossover frequency (f_{xo}) for the transition from negative to positive dielectrophoresis (DEP) behavior to enable strain-based separations.[19] In the current study, we focus on measuring alterations in the cell envelope capacitance of the HTCD strain, VPI10463, after co-culture with the NTCD strain, VPI11186, or with various cell-free supernatants of this strain (NTCD-S, with HTCD-S serving as the control). Considering the DEP spectra for HTCD cultured in NTCD-

S versus HTCD cultured in HTCD-S (Figure 3a), a small shift toward higher frequencies is apparent within the spectra,
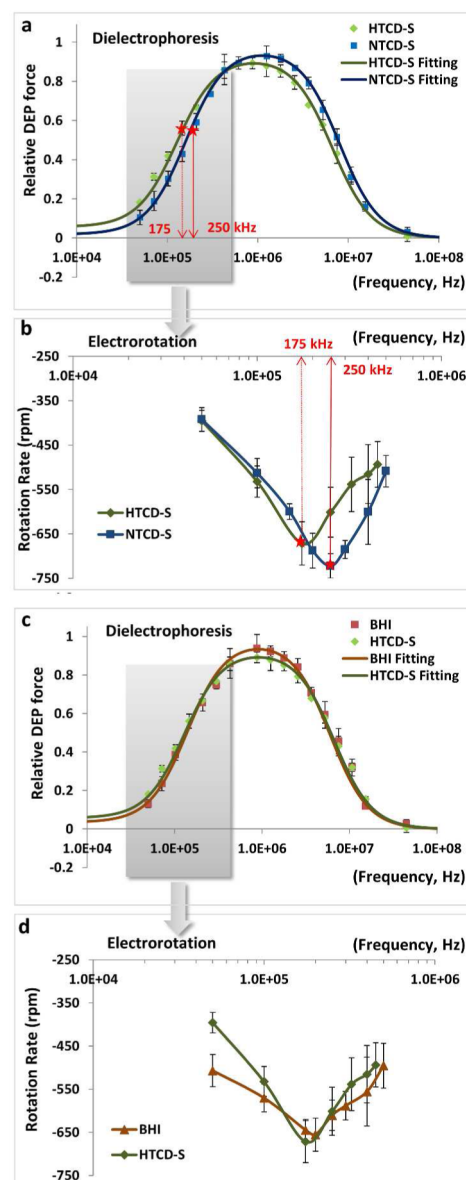
Figure 3. HTCD cultured in HTCD-S versus in NTCD-S, analyzed on the basis of (a) DEP spectra (50 kHz−45 MHz) and (c) ROT spectra (50 kHz−500 kHz), with the respective control measurement of HTCD cultured in BHI versus in HTCD-S: (b) DEP spectra and (d) ROT spectra. The DEP responses are fit to eq 2 (Supporting Information) to compute *C. difficile* electrophysiology (Table 1), with red star symbols on plots indicating the particular frequencies of DEP inflection (a), which correspond to the frequencies of the highest counter-field rotation rate (b). See ROT video: ROT2.mov in Supporting Information.

whereas no discernible shifts are apparent between the spectra for HTCD cultured in HTCD-S versus the control of HTCD cultured in BHI media (Figure 3c). To better delineate these differences, we measured the electro-rotation (ROT) spectra for the respective HTCD cells (full range in Figure S2b) because the pDEP inflection frequency is seen as a peak in the counter-field rotation rate, thereby sensitively discerning the spectral shifts. As shown in Figure 3b, the highest rotation rate for HTCD cultured in HTCD-S occurs at 175 kHz, whereas
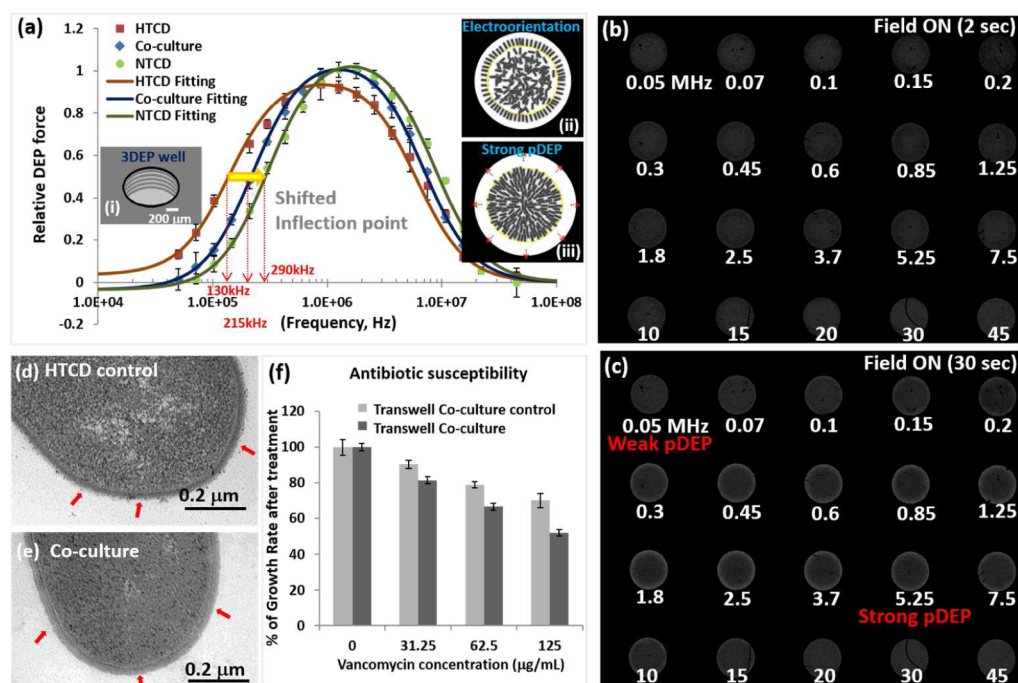
Figure 4. (a) DEP spectra (50 kHz−45 MHz) of HTCD co-cultured in NTCD versus in the respective co-culture control and the pure NTCD culture (video DEP1.mov in SI). The fitted DEP response under each culture condition (using eq 2 Supporting Information) is applied to compute dielectric parameters of the *C. difficile* cell envelope and cytoplasm (Table 1). Schematic images show (i) rings of conducting electrode strips patterned inside the wall of a 3D well; (ii) the cells electro-orient to form a dark band at the edge at early time points; (iii) after 30 s of field, pDEP causes a clear band at the electrode edge (from bands 6−9, with the yellow circle indicating band 6). Representative light intensity images of *C. difficile* in the 3DEP well device at the indicated frequencies due to electro-orientation after 2 s (b) and pDEP after 30 s (c) are used to determine DEP spectra. Transmission electron microscopy images of (d) the HTCD control and (e) HTCD co-cultured with NTCD (arrows indicate S-layer-induced features). (f) Antibiotic susceptibility of HTCD co-cultured with NTCD versus the co-cultured HTCD control (growth rates normalized to those of untreated cells; i.e., 0 *μ*g/mL vancomycin treatment has a 100% growth rate).

the highest rotation rate for HTCD cultured in NTCD-S occurs at 250 kHz, somewhat consistent with the DEP spectral shifts in Figure 3a. Furthermore, consistent with the DEP spectra in Figure 3c, no shifts are apparent in the ROT spectra for HTCD cultured in HTCD-S versus the control (HTCD cultured in BHI media (Figure 3d).

In contrast to the small shifts in DEP spectra for HTCD after culture within the cell-free NTCD supernatant, the upshifting of the DEP inflection point to higher frequencies is much clearer for HTCD after transwell co-culture with NTCD versus with the HTCD strain (co-culture control) so that the co-cultured HTCD cells show a dispersion behavior that approaches that of the NTCD strain (Figure 4a). Because *C. difficile* has an ellipsoidal structure with a high eccentricity (major to minor axis ratio of ∼6), the cell electro-orients over the first few seconds, followed by strong pDEP behavior of the electro-oriented cells that are close to the high-field region (i.e., electrode edges), as indicated in Figure 4a within insets (i) and (ii). A typical image of the field dispersion spectra for co-cultured HTCD cells shows that a dark band due to electro-oriented cells is formed at the electrode-edge within the first few seconds of the electric field application (Figure 4b). The same image after 30 s of electric field (Figure 4c) shows strong pDEP in the 0.3−10 MHz range and weak pDEP at lower (<0.3 MHz) and higher frequencies (>10 MHz), with the brighter electrode edge indicating successively higher pDEP levels.

The DEP spectra of the HTCD cells in Figures 3 and 4, acquired from spatiotemporal variations in light scattering

across the 3D electrode well,[28] were fit to a two-shell ellipsoidal dielectric model[29] to compute the cell envelope capacitance ($C_{envelope}$) and conductivity and permittivity of the cytoplasm (σ_{cyto} and ε_{cyto}), with fits to the model showing an R^2 of 0.98 or higher, as per Table 1. The cell envelope capacitance (in mF/

Table 1. Dielectric Parameters of the Cell Envelope ($C_{envelope}$ in mF/m²) and Cytoplasm (σ_{cyto} in S/m and ε_{cyto}) of *C. difficile* (HTCD) in Various Culture Media by Fitting the Recorded DEP Spectra of Figure 3a (in NTCD-S), Figure 3b (in HTCD-S), and Figure 4a (Co-Cultured in HTCD) to an Ellipsoidal Two-Shell Model[a]

	BHI	HTCD-S	NTCD-S	co-culture	NTCD
$C_{envelope}$(mF/m²)	0.9716	0.9933	0.6879	0.4347	0.3409
ε_{cyto}	65	65	65	60	65
σ_{cyto}(S/m)	0.48	0.50	0.52	0.55	0.6

[a]Details in Table S2 of the Supporting Information.

m² units) decreases from 0.97 for HTCD in standard BHI to 0.68 for HTCD cultured in NTCD-S and further down to 0.43 for HTCD after transwell co-culture in NTCD, with no significant differences between HTCD cultured in HTCD-S versus HTCD cultured in BHI. It is noteworthy that the effective cytoplasmic conductivity and permittivity of HTCD remain somewhat unchanged, highlighting that the chief differences arise in the capacitance of the cell envelope.

To understand the underlying mechanism that causes this >50% reduction in the cell envelope capacitance of the HTCD cells after transwell co-culture with NTCD cells, we examined

the respective cell wall morphologies using transmission electron microscopy. As per the images shown in Figure 4d versus Figure 4e, the cell-wall surface of HTCD co-cultured with NTCD shows a significantly lower roughness (Figure 4e) versus that of the HTCD control (Figure 4d), which correlates with its lower capacitance. The less electron-dense areas in the cytoplasm region of the image, likely due to nucleoids,[35] do not exhibit substantial differences between the different cell types. Alterations in the surface roughness of the microbial cell wall have previously been correlated to variations in S-layer composition.[34] For the case of *C. difficile*, such S-layer variations between strain types typically cause significant alterations in their colonization ability, as also apparent within our results that show significantly lowered host cell adherence for the NTCD versus the HTCD strain studied herein (Figure 2c). Hence, we suggest that the significant reduction in the colonization ability of HTCD after co-culture with NTCD or after culture in NTCD-S can be related to the alterations in its cell-wall surface structure, as apparent from the smoother morphology of their cell wall surface, which can be discerned rather easily by following the shifts in the DEP spectra due to cell envelope capacitance. Hence, rather than applying time-consuming and cumbersome adhesion assays to follow alterations in the colonization ability of HTCD strains after co-culture with probiotic microbial strains, we suggest that DEP methods can discern these alterations within a few minutes on the basis of their cell envelope capacitance. Finally, we compare the antibiotic susceptibility of HTCD co-cultured with NTCD versus that of the co-cultured HTCD control by comparing the growth rates after each vancomycin treatment (of varying levels) normalized to those of untreated cells (i.e., 0 μg/mL vancomycin-treated cells have a 100% growth rate). On the basis of Figure 4f, it is apparent that HTCD co-cultured with NTCD becomes significantly more susceptible to vancomycin treatment because of the lower % of untreated cells at each of the three investigated vancomycin levels. We attribute this increase in the antibiotic susceptibility of co-cultured HTCD to its interactions with the secreted extracellular factors from NTCD, which seem to alter the cell functionality, as measured by its growth rate, toxin production, and colonization ability (Figure 2a−c), and which correlates to the altered cell-envelope capacitance.

CONCLUSIONS

Cell envelope capacitance measurements are presented as a rapid and quantitative methodology to probe S-layer-induced alterations in the *C. difficile* cell wall region for applications toward probing the inhibition of its host cell colonization ability after co-culture with probiotic microorganisms. First, co-culture of the HTCD strain, VPI10463, with the NTCD strain, VPI11186, is shown to have a strong inhibitory effect on the colonization ability of HTCD (Figure 2c), with successively milder inhibitory effects on its toxin production levels (Figure 2b) and growth rate (Figure 2a), whereas upon culture of the HTCD strain with cell-free NTCD supernatant this inhibitory effect is apparent only at a modest level with respect to the colonization ability of HTCD (Figure 2c). We attribute this observation to the dynamic contact of HTCD cells with freshly secreted extracellular factors from NTCD within the co-culture system, whereas for HTCD culture in cell-free NTCD supernatant the contact is with isolated extracellular factors from one particular time point. On the basis of comparing the influence of heat treatment on the cell-free supernatant of

NTCD (NTCD-S) versus HTCD (HTCD-S), we are able to infer the role that thermolabile extracellular factors present in the NTCD-S play in the inhibitory effect on HTCD cells (Figure 2d). Next, through monitoring variations in field screening by the HTCD cell envelope due to its capacitance, we infer a high level of frequency upshifting for inflection toward positive DEP behavior for HTCD co-cultured with NTCD versus that of its control. The DEP spectra are fit to a two-shell dielectric model for an ellipsoidal particle (Table 1 and Table S2, SI) to infer >50% reduction in its cell envelope capacitance (Figure 4a). On the other hand, a milder level of inhibition for HTCD cultured in NTCD-S is apparent from a lower degree of upshifting in the inflection of its spectra that can be fit to infer an ∼30% reduction in its cell envelope capacitance (Figure 3). This reduction in the cell envelope capacitance and effective permittivity of the cell wall region are consistent with the alterations in cell wall morphology that reveal a significant reduction in cell wall roughness after HTCD co-culture with NTCD. Finally, we observe a significant increase in the antibiotic susceptibility of co-cultured HTCD versus that of the control, which is attributed to arise from interactions of HTCD with the secreted extracellular factors from NTCD during the co-culture that alters the cell functionality. We envision a diagnostic platform based on cell envelope capacitance to rapidly screen for particular probiotic combinations that inhibit the colonization ability of co-cultured HTCD versus current methods based on cumbersome adhesion assays, thereby enabling the study of a larger number of inhibitory permutations.

ASSOCIATED CONTENT

Ⓢ Supporting Information

The Supporting Information is available free of charge on the ACS Publications website at DOI: 10.1021/acsinfec-dis.6b00050.

> Viability of *C. difficile* in altered buffer, representative measurements of cell wall thickness from TEM images of HTCD and NTCD strains, spatial distribution of the electric field during ROT, wide-band ROT spectra for highly toxigenic *C. difficile*, representative sets of images showing HTCD electrororotation, dielectric parameters obtained by fitting DEP spectra to a two-shell ellipsoidal model, and the fitting of DEP spectra to compute dielectric parameters (PDF)
>
> Time-resolved images of positive DEP trapping of HTCD co-cultured with NTCD as acquired within a 3DEP well device (MPG)
>
> Time-resolved images of electro-rotation of HTCD indicating differences in rotation rate with frequency (MPG)

AUTHOR INFORMATION

Corresponding Author

*Fax: +1-434-924-8818. E-mail: nswami@virginia.edu.

Notes

The authors declare no competing financial interest.

Moore on microbiological analysis, as well as assistance from Michael P. Hughes and Kai Hoettges at DEPtech for co-development of the 3DEP for bacterial analysis.

■ REFERENCES

(1) Rupnik, M., Wilcox, M. H., and Gerding, D. N. (2009) Clostridium difficile infection: new developments in epidemiology and pathogenesis. *Nat. Rev. Microbiol.* 7 (7), 526−36.

(2) Burke, K. E., and Lamont, J. T. (2014) Clostridium difficile infection: a worldwide disease. *Gut Liver* 8 (1), 1−6.

(3) Parkes, G. C., Sanderson, J. D., and Whelan, K. (2009) The mechanisms and efficacy of probiotics in the prevention of Clostridium difficile-associated diarrhoea. *Lancet Infect. Dis.* 9 (4), 237−44.

(4) Johnston, B. C., Ma, S. S., Goldenberg, J. Z., Thorlund, K., Vandvik, P. O., Loeb, M., and Guyatt, G. H. (2012) Probiotics for the prevention of Clostridium difficile-associated diarrhea: a systematic review and meta-analysis. *Ann. Intern. Med.* 157 (12), 878−88.

(5) Trejo, F. M., De Antoni, G. L., and Perez, P. F. (2013) Protective effect of bifidobacteria in an experimental model of Clostridium difficile associated colitis. *J. Dairy Res.* 80 (3), 263−9.

(6) Bolla, P. A., Carasi, P., Bolla, M. D., De Antoni, G. L., and Serradell, M. D. (2013) Protective effect of a mixture of kefir-isolated lactic acid bacteria and yeasts in a hamster model of Clostridium difficile infection. *Anaerobe* 21, 28−33.

(7) Trejo, F. M., Minnaard, J., Perez, P. F., and De Antoni, G. L. (2006) Inhibition of Clostridium difficile growth and adhesion to enterocytes by Bifidobacterium supernatants. *Anaerobe* 12 (4), 186−193.

(8) Banerjee, P., Merkel, G. J., and Bhunia, A. K. (2009) Lactobacillus delbrueckii ssp bulgaricus B-30892 can inhibit cytotoxic effects and adhesion of pathogenic Clostridium difficile to Caco-2 cells. *Gut Pathog.* 1, 8.

(9) Trejo, F. M., Perez, P. F., and De Antoni, G. L. (2010) Co-culture with potentially probiotic microorganisms antagonises virulence factors of Clostridium difficile in vitro. *Antonie van Leeuwenhoek* 98 (1), 19−29.

(10) Woo, T. D. H., Oka, K., Takahashi, M., Hojo, F., Osaki, T., Hanawa, T., Kurata, S., Yonezawa, H., and Kamiya, S. (2011) Inhibition of the cytotoxic effect of Clostridium difficile in vitro by Clostridium butyricum MIYAIRI 588 strain. *J. Med. Microbiol.* 60 (11), 1617−1625.

(11) Villano, S. A., Seiberling, M., Tatarowicz, W., Monnot-Chase, E., and Gerding, D. N. (2012) Evaluation of an oral suspension of VP20621, spores of nontoxigenic Clostridium difficile strain M3, in healthy subjects. *Antimicrob. Agents Chemother.* 56 (10), 5224−9.

(12) Gerding, D. N., Meyer, T., Lee, C., Cohen, S. H., Murthy, U. K., Poirier, A., Van Schooneveld, T. C., Pardi, D. S., Ramos, A., Barron, M. A., Chen, H. Z., and Villano, S. (2015) Administration of Spores of Nontoxigenic Clostridium difficile Strain M3 for Prevention of Recurrent C difficile Infection A Randomized Clinical Trial. *Jama-J. Am. Med. Assoc* 313 (17), 1719−1727.

(13) Sambol, S. P., Merrigan, M. M., Tang, J. K., Johnson, S., and Gerding, D. N. (2002) Colonization for the prevention of Clostridium difficile disease in hamsters. *J. Infect. Dis.* 186 (12), 1781−1789.

(14) Youngster, I., Russell, G. H., Pindar, C., Ziv-Baran, T., Sauk, J., and Hohmann, E. L. (2014) Oral, capsulized, frozen fecal microbiota transplantation for relapsing Clostridium difficile infection. *Jama* 312 (17), 1772−8.

(15) Fagan, R. P., and Fairweather, N. F. (2014) Biogenesis and functions of bacterial S-layers. *Nat. Rev. Microbiol.* 12 (3), 211−22.

(16) Merrigan, M. M., Venugopal, A., Roxas, J. L., Anwar, F., Mallozzi, M. J., Roxas, B. A., Gerding, D. N., Viswanathan, V. K., and Vedantam, G. (2013) Surface-layer protein A (SlpA) is a major contributor to host-cell adherence of Clostridium difficile. *PLoS One* 8 (11), e78404.

(17) Reynolds, C. B., Emerson, J. E., de la Riva, L., Fagan, R. P., and Fairweather, N. F. (2011) The Clostridium difficile Cell Wall Protein CwpV is Antigenically Variable between Strains, but Exhibits Conserved Aggregation-Promoting Function. *PLoS Pathog.* 7 (4), e1002024.

(18) Spigaglia, P., Barketi-Klai, A., Collignon, A., Mastrantonio, P., Barbanti, F., Rupnik, M., Janezic, S., and Kansau, I. (2013) Surface-layer (S-layer) of human and animal Clostridium difficile strains and their behaviour in adherence to epithelial cells and intestinal colonization. *J. Med. Microbiol.* 62, 1386−1393.

(19) Su, Y. H., Warren, C. A., Guerrant, R. L., and Swami, N. S. (2014) Dielectrophoretic monitoring and interstrain separation of intact Clostridium difficile based on their S(Surface)-layers. *Anal. Chem.* 86 (21), 10855−63.

(20) Hywel Morgan, N. G. G. In *AC Electrokinetics: Colloids and Nanoparticles*; Research Studies Press Ltd., 2002; p 250.

(21) Pohl, H. A. *Dielectrophoresis: The Behavior of Neutral Matter in Nonuniform Electric Fields*; Cambridge University Press: Cambridge, 1978.

(22) Su, Y. H., Tsegaye, M., Varhue, W., Liao, K. T., Abebe, L. S., Smith, J. A., Guerrant, R. L., and Swami, N. S. (2014) Quantitative dielectrophoretic tracking for characterization and separation of persistent subpopulations of Cryptosporidium parvum. *Analyst* 139 (1), 66−73.

(23) Farmehini, V., Rohani, A., Su, Y.-H., and Swami, N. (2014) Wide bandwidth power amplifier for frequency-selective insulator-based dielectrophoresis. *Lab Chip* 14 (21), 4183−4187.

(24) Goater, A. D., and Pethig, R. (1998) Electrorotation and dielectrophoresis. *Parasitology* 117 (Suppl), S177−S189.

(25) Rohani, A., Varhue, W., Su, Y. H., and Swami, N. S. (2014) Electrical tweezer for highly parallelized electro-rotation measurements over a wide frequency bandwidth. *Electrophoresis* 35, 1795−1802.

(26) Rohani, A., Varhue, W., Su, Y. H., and Swami, N. S. (2014) Quantifying spatio-temporal dynamics of biomarker pre-concentration and depletion in microfluidic systems by intensity threshold analysis. *Biomicrofluidics* 8 (5), 052009.

(27) Broche, L. M., Hoettges, K. F., Ogin, S. L., Kass, G. E. N., and Hughes, M. P. (2011) Rapid, automated measurement of dielectrophoretic forces using DEP-activated microwells. *Electrophoresis* 32 (17), 2393−2399.

(28) Mulhall, H. J., Cardnell, A., Hoettges, K. F., Labeed, F. H., and Hughes, M. P. (2015) Apoptosis progression studied using parallel dielectrophoresis electrophysiological analysis and flow cytometry. *Integr Biol-Uk* 7 (11), 1396−1401.

(29) Hawkins, B. G., Huang, C., Arasanipalai, S., and Kirby, B. J. (2011) Automated dielectrophoretic characterization of Mycobacterium smegmatis. *Anal. Chem.* 83 (9), 3507−15.

(30) Jones, T. B. *Electromechanics of Particles*; Cambridge University Press: Cambridge, 1995.

(31) Perfumo, A., Elsaesser, A., Littmann, S., Foster, R. A., Kuypers, M. M. M., Cockell, C. S., and Kminek, G. (2014) Epifluorescence, SEM, TEM and nanoSIMS image analysis of the cold phenotype ofClostridium psychrophilumat subzero temperatures. *FEMS Microbiol. Ecol.* 90 (3), 869−882.

(32) Milo, R., and Phillips, R. *Cell Biology by the Numbers*; Garland Science: New York, 2016.

(33) Inoue, S., Lee, H.-B., Becker, A. L., Weigel, K. M., Kim, J.-H., Lee, K.-H., Cangelosi, G. A., and Chung, J.-H. (2015) Dielectrophoretic characterization of antibiotic-treated Mycobacterium tuberculosis complex cells. *Anal. Bioanal. Chem.* 407 (25), 7673−7680.

(34) Sekot, G., Posch, G., Messner, P., Matejka, M., Rausch-Fan, X., Andrukhov, O., and Schaffer, C. (2011) Potential of the Tannerella forsythia S-layer to Delay the Immune Response. *J. Dent. Res.* 90 (1), 109−114.

(35) Thanbichler, M., Wang, S. C., and Shapiro, L. (2005) The bacterial nucleoid: A highly organized and dynamic structure. *J. Cell. Biochem.* 96 (3), 506−21.